JOURNAL OF AGRICULTURAL AND FOOD CHEMISTRY

Article

pubs.acs.org/JAFC

Surface Properties and Chemical Composition of Corncob and Miscanthus Biochars: Effects of Production Temperature and Method

Alice Budai,[*,†,‡] Liang Wang,[§] Morten Gronli,[∥] Line Tau Strand,[‡] Michael J. Antal, Jr.,[⊥] Samuel Abiven,[#] Alba Dieguez-Alonso,[△] Andres Anca-Couce,[▽,△] and Daniel P. Rasse[†]

[†]Soil and Environment Division, Bioforsk − Norwegian Institute for Agricultural and Environmental Research, Frederik A. Dahl vei 20, 1430 Ås, Norway

[‡]Department of Plant and Environmental Sciences, Norwegian University of Life Sciences, Box 5003, 1432 Ås, Norway

[§]Department of Thermal Energy, SINTEF Energy Research, Sem Saelands vei 11, 7465 Trondheim, Norway

[∥]Department of Energy and Process Engineering, Norwegian University of Science and Technology, Kolbjørn Hejes vei 1B, 7491 Trondheim, Norway

[⊥]Hawaii Natural Energy Institute, School of Ocean and Earth Sciences and Technology, University of Hawaii at Manoa, Honolulu, Hawaii 96822, United States

[#]Department of Geography, University of Zurich, Winterthurerstrasse 190, 8057 Zurich, Switzerland

[△]Institute of Energy Engineering, Chair for Energy Process Engineering and Conversion Technologies for Renewable Energies, Technische Universitat Berlin, Fasanenstrasse 89, 10623 Berlin, Germany

[▽]Institute for Process and Particle Engineering, Graz University of Technology, Inffeldgasse 21b, 8010 Graz, Austria

Supporting Information

ABSTRACT: Biochar properties vary, and characterization of biochars is necessary for assessing their potential to sequester carbon and improve soil functions. This study aimed at assessing key surface properties of agronomic relevance for products from slow pyrolysis at 250−800 °C, hydrothermal carbonization (HTC), and flash carbonization. The study further aimed at relating surface properties to current characterization indicators. The results suggest that biochar chemical composition can be inferred from volatile matter (VM) and is consistent for corncob and miscanthus feedstocks and for the three tested production methods. High surface area was reached within a narrow temperature range around 600 °C, whereas cation exchange capacity (CEC) peaked at lower temperatures. CEC and pH values of HTC chars differed from those of slow pyrolysis biochars. Neither CEC nor surface area correlated well with VM or atomic ratios. These results suggest that VM and atomic ratios H/C and O/C are good indicators of the degree of carbonization but poor predictors of the agronomic properties of biochar.

KEYWORDS: *hydrothermal carbonization, flash carbonization, slow pyrolysis, ^{13}C, cation exchange capacity (CEC), surface area*

INTRODUCTION

Biochar is charcoal specifically produced for soil application with the aim of increasing C sequestration and improving soil fertility.[1] It is produced through thermal treatment of biomass under limited or no oxygen using conversion processes including slow and fast pyrolysis, flash carbonization, and gasification. Other low-temperature treatments such as torrefaction and HTC produce torrefied biomass and hydrochar.[2,3] Heat treatment induces successive chemical reactions of biomass materials such as cleavage and polymerization reactions,[2] with energy supply rate, pressure, catalytic inorganic impurities, and carrier gas composition influencing the extent of the reactions.[4,5] Among influential process parameters, the maximum temperature reached during the pyrolysis process is the most critical one to influence biochar yields and properties.[5] This temperature refers to the highest treatment temperature (HTT) for the raw feedstock during the biochar production process. Increasing HTT results in a progressive loss of H (hydrogen) and O (oxygen) and a comparative enrichment in C (carbon).[6] The resultant C-rich biochar is more resistant to microbial degradation as compared to fresh biomass and holds promise for mitigating climate change through sequestering C in soil.[7]

Biochar also has potential to improve properties of agricultural soils.[8] An overall increase in biomass production is observed when biochar is added to agricultural soil. However, variability in individual studies is large because of differences in soil conditions such as pH and texture[9] and also because of differences in the types of biochar used in the experiments. A full mechanistic understanding of how biochar increases soil fertility is not yet available,[10,11] but key agronomic functions of biochar include water retention, nutrient retention, and liming effect.[2] These functions are borne by biochar surface properties such as high surface area (SA), high pH, and the potential to increase the cation exchange capacity (CEC) of soil.[3] Being a porous material, biochar increases soil water-holding capacity and affects the microbial environment.[12] Microbial populations and their functions are also affected by high-pH biochars

Received: November 13, 2013
Accepted: April 10, 2014
Published: April 10, 2014

through the liming effect.[9,13] In general, both pH and CEC of biochar influence the availability of nutrients to soil microbes and plants,[2] and soils amended with biochar or black carbon generally display higher CEC and SA than equivalent biochar-free soils.[3,14,15] Intensive studies showed biochar amendments increase soil pH and have significant consequent effects on plant growth.[9] On the other hand, some studies reported no or only slight changes in soil pH, CEC, and SA with biochar amendment, which is attributed to specific soil or biochar properties.[2,16] Detailed characterization of biochar is essential for forecasting and maximizing impacts of biochar amendment on soil properties.

Biochar properties have not yet been fully linked to production parameters, making the design of agronomic biochars a challenge.[3] Reasons for why this link does not yet exist may include the complexity of pyrolysis processes, which can be influenced by many factors. In addition, process parameters are difficult to control in large reactors, enhancing the complexity of biochar production processes and the heterogeneity of products.[2] Biochar properties can be assessed via a combination of rather simpler proxy-type analyses and advanced analytical techniques. Proxy-type analyses are therefore more practical also from a user standpoint as users may wish to mix various biochars for a homogeneous product. The International Biochar Initiative and a panel of experts have identified a proxy for the assessment of biochar stability,[17] and the characterization of other biochar properties will likely also rely on proxy-type analyses.

Robust assessment of biochar properties requires the existence of simple relationships, preferably linear, between production conditions or proxy measurements and complex properties. Several studies suggest that such simple relationships exist for critical chemical composition and surface property indicators. Increasing pyrolysis temperature has been reported to result in continuous increases in pH, CEC,[18] and SA.[19] However, not all studies agree with these findings. Surface area has been reported to reach a peak value and then decrease at higher HTT for both wood and wheat biochars.[20,21] Similarly, CEC has also been reported to display a localized maximum at midrange HTT.[22] Many studies use few biochar samples along a temperature continuum, and considerable uncertainty remains as to our ability to predict surface properties on the basis of biochar production methods. Here, our objective was to obtain detailed responses of selected biochar properties to HTT for three pyrolysis methods. For this, we used a ca. 15-point temperature series in slow pyrolysis of two feedstocks each as well as HTC hydrochars and flash carbonization biochars produced from the same feedstocks. This allowed us to obtain an extensive sample set for testing the hypothesis that surface properties follow simple relationships with HTT production conditions and can be predicted from chemical composition indicators.

MATERIALS AND METHODS

Carbonization. Three production methods were tested: slow pyrolysis, flash carbonization, and HTC treatment. Identical feedstocks were used for slow pyrolysis and HTC treatment: chaffed biomass of grass (*Miscanthus giganteus*) and corncob from maize (*Zea mays*) grown in Serbia (ZP Maize Hybrid 505). In addition to slow pyrolysis and HTC, flash carbonization was conducted on a batch of corncobs from Waimanalo Farm in Hawaii. In total, 34 biochars were produced (Table 1). In the present study, we used feedstock derived from plants using the C4 photosynthetic pathway, that is, miscanthus and maize. The C4 feedstock has a distinctive ^{13}C signature from that of soil organic matter, which we used in a parallel study on estimating the stability of biochar C structures in soil. Within the limited range of C4 feedstocks, miscanthus and corncob are good candidates for biochar production. Miscanthus is a high-yielding bioenergy crop requiring minimal soil preparation, and biochar prepared from it has potential for being a silicon fertilizer.[23] Corncob, in comparison, is a crop residue, which needs to be valorized and does not compete for land with food production.

Slow pyrolysis was performed in a muffle furnace at target temperatures ranging from 235 to 800 °C with a heating rate of 2.5 °C min^{-1}. Pyrolysis HTTs were selected to produce biochars containing a wide range of VM content. To aid the selection process, a set of preliminary analyses were conducted on the feedstocks using a thermogravimetric analyzer (SDT Q600, TA Instruments, New Castle, DE, USA). Fourteen miscanthus and 17 corncob biochars were generated through slow pyrolysis of chaffed miscanthus and corncobs cut into ca. 5 mm slices. A detailed procedure for the pyrolysis is provided by Wang et al.[24] Feedstock was dried at 105 °C for 24 h and

Table 1. Elemental Compositions of Corncob (CC) and Miscanthus (MS) Exposed to Hydrothermal Carbonization (HTC), Slow Pyrolysis (Slow), and Flash Carbonization (Flash) at Designated Highest Treatment Temperatures (HTT)[a]

feedstock-method	HTT (°C)	C (%)	N (%)	O (%)	H (%)
CC	105	47.7 (0.7)	0.4 (0.0)	56.5 (0.3)	6.5 (0.0)
CC-Flash	600	83.2 (1.0)	1.4 (0.1)	8.7 (0.2)	2.1 (0.1)
CC-HTC	230	59.9 (0.8)	0.4 (0.0)	40.7 (0.3)	6.0 (0.1)
CC-Slow		67.0 (0.6)	0.5 (0.0)	29.0 (0.2)	5.1 (0.1)
CC-Slow	377	74.1 (0.3)	0.6 (0.1)	20.6 (0.2)	4.5 (0.1)
CC-Slow	372	71.9 (0.8)	0.5 (0.0)	26.1 (0.5)	4.8 (0.1)
CC-Slow	369	74.2 (0.7)	0.6 (0.1)	23.3 (0.2)	4.6 (0.1)
CC-Slow	357	74.2 (1.0)	0.6 (0.0)	23.5 (0.1)	4.8 (0.1)
CC-Slow	386	76.2 (0.9)	0.7 (0.0)	20.6 (0.3)	4.2 (0.1)
CC-Slow	416	78.8 (1.2)	0.5 (0.0)	17.6 (0.2)	3.9 (0.1)
CC-Slow	440	80.1 (0.9)	0.6 (0.0)	15.0 (0.1)	3.5 (0.1)
CC-Slow	485	83.5 (0.7)	0.7 (0.0)	11.1 (0.3)	3.2 (0.1)
CC-Slow	562	86.8 (0.8)	0.8 (0.0)	9.1 (0.2)	2.7 (0.1)
CC-Slow	576	86.9 (0.8)	0.8 (0.0)	6.6 (0.3)	2.5 (0.1)
CC-Slow	687	90.1 (0.7)	1.0 (0.1)	4.8 (0.2)	1.8 (0.1)
CC-Slow	693	89.4 (0.4)	0.9 (0.1)	5.6 (0.1)	1.7 (0.1)
CC-Slow	796	91.5 (0.4)	1.0 (0.0)	4.6 (0.1)	1.0 (0.1)
MS	105	47.9 (0.9)	0.2 (0.0)	51.8 (0.5)	6.1 (0.1)
MS-HTC	230	62.2 (0.6)	0.2 (0.0)	35.4 (0.3)	5.6 (0.1)
MS-Slow	272	56.1 (1.5)	0.3 (0.0)	35.2 (0.1)	6.0 (0.1)
MS-Slow	235	46.1 (1.4)	0.3 (0.0)	40.1 (0.1)	5.4 (0.3)
MS-Slow	369	66.6 (0.7)	0.4 (0.0)	22.3 (0.5)	4.5 (0.1)
MS-Slow	385	67.7 (0.8)	0.4 (0.0)	19.7 (0.5)	4.1 (0.2)
MS-Slow	400	63.7 (1.4)	0.4 (0.0)	16.3 (0.3)	3.4 (0.1)
MS-Slow	406	70.9 (0.8)	0.4 (0.0)	17.2 (0.1)	3.8 (0.1)
MS-Slow	411	73.2 (1.8)	0.4 (0.0)	15.7 (0.3)	3.5 (0.1)
MS-Slow	406	72.0 (0.6)	0.4 (0.0)	18.9 (0.3)	4.2 (0.1)
MS-Slow	416	73.6 (2.1)	0.4 (0.0)	12.8 (0.3)	3.3 (0.1)
MS-Slow	442	73.6 (1.6)	0.4 (0.0)	12.1 (0.2)	3.1 (0.1)
MS-Slow	503	64.5 (4.1)	0.4 (0.1)	9.7 (0.3)	2.4 (0.2)
MS-Slow	464	75.3 (2.9)	0.5 (0.1)	11.2 (0.2)	3.1 (0.1)
MS-Slow	600	71.9 (3.3)	0.5 (0.1)	5.5 (0.5)	2.0 (0.1)
MS-Slow	590	77.3 (3.4)	0.5 (0.0)	6.8 (0.2)	2.2 (0.1)
MS-Slow	693	84.6 (2.1)	0.7 (0.1)	6.1 (0.3)	1.7 (0.1)
MS-Slow	682	75.6 (2.4)	0.6 (0.0)	5.0 (0.3)	1.5 (0.1)
MS-Slow	790	83.7 (1.6)	0.8 (0.1)	5.8 (0.2)	0.8 (0.1)

[a]Standard deviations are shown in parentheses for analytical replicates; $n = 5$ (C, H, and N) and $n = 3$ (O).

weighed prior to loading into a 1 L stainless steel retort. The retort, equipped with thermocouples placed at the center, bottom, side, and front, was then covered with a lid and placed into a furnace. The retort was purged for 1 h to create an inert atmosphere, and a constant flow of N_2 was maintained at 2 L min^{-1} during pyrolysis. After the desired final temperature was achieved, heat supply from the furnace was stopped and the sample cooled slowly to room temperature. To present a more representative sample history, we consistently reported measured HTTs from the average of the four thermocouples in the retort instead of set temperatures for the furnace. Exothermic reactions occurred during slow pyrolysis in the approximate temperature range of 250−400 °C, and actual HTTs measured by the thermocouples were higher than the set temperatures (Figure 1). As a result, few

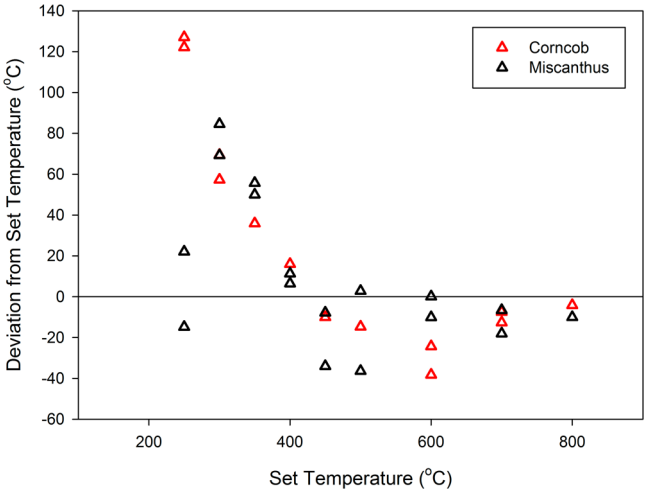

Figure 1. Deviation of measured highest treatment temperature (HTT) from oven set temperatures during slow pyrolysis.

samples are recorded at pyrolysis temperatures around 350 °C, at which the pyrolysis process is difficult to halt. At pyrolysis temperatures of ≥450 °C, measured HTTs in the retort did not exceed target values.

HTC treatment of corncob and miscanthus was performed in a 1 L steel autoclave (Anton Paar), immersed in water, and then heated at 230 °C for 6 h under autogenous pressure. After cooling, the autoclaves were opened, and the resultant hydrochar was removed from the aqueous dispersion by vacuum filtration. The resulting fine powder was dried at 40 °C. Because the hydrochar yield was not directly measured at the time of production, it was estimated from the literature[25] for the purpose of comparison.

Flash carbonization was performed on corncob to produce biochar according to the method of Antal et al.[26] The reaction lasted 20 min in a vessel pressurized to 0.8−3.4 MPa with air. Electric heating coils at the bottom of the pressure vessel ignited the lower portion of the biomass. After 360 s, compressed air was delivered to the top of the pressure vessel and flowed through the packed bed of feedstock to sustain the carbonization process. Pressure within the reactor was maintained at the specified range. After sufficient air was delivered to carbonize the corncob, air flow was halted and the reactor cooled overnight. The charcoal was removed from the reactor and allowed to equilibrate under a fume hood for 2 days.

All samples were crushed through a 2 mm sieve, and subsamples were subsequently ground for greater homogeneity with a ball mill for 3 min at 20 s^{-1} shaking frequency (MM 200, Retsch GmbH, Haan, Germany). The samples were stored in airtight bags until analyzed.

Physical and Chemical Analyses. Proximate analysis of the biomass feedstock was performed according to American Society for Testing and Materials (ASTM) methods E 871 and 872 with modifications as described by Wang et al.[24] In brief, ash content was determined according to ASTM method D 1102. The fixed carbon contents of the samples were calculated by difference between 100% and the sum of measured VM and ash contents. The VM content of the charcoal products was determined according to ASTM method D 1762-84 with the modification that samples were directly placed at the rear of a furnace for 6 min at 950 °C without preheating.[24]

Elemental composition (C, H, N) of the samples was determined on 50−100 mg samples by dry combustion using a Leco CHN1000 analyzer and coal reference material (Leco Corp., St. Joseph, MI, USA). Oxygen was determined on 2 mg samples dried at 90 °C with a TruSpec Makro analyzer and O add-on module (Leco Corp.). Results are reported on a dry weight basis. pH was determined in a biochar/water volume ratio of 1:10 using a combination Orion pH electrode (SA 720, Allometrics, Inc., Baton Rouge, LA, USA).

Potential CEC was determined by using a modified ammonium acetate compulsory displacement method. Soluble ions, which can constitute an artifact, were removed through five successive leachings of 0.5 g samples with 20 mL of deionized water. Preliminary analyses were conducted on the initial water leachates to determine the most important cations present following the method of Gaskin et al.[27] Analysis of the water leachates suggested that between 97 and 100% of the extractable/exchangeable cations were covered by five cations. After the removal of soluble ions with water, remaining cations were displaced using 50 mL of 1 M ammonium acetate buffered to pH 7. CEC was calculated by the sum of the cations Ca, Mg, K, and Na in the ammonium acetate percolate. H^+, determined by titration, was included when the pH was <7. Additional preliminary analyses involved CEC determination on a subset of samples exposed to pretreatment with acid. Acid washing is expected to remove carbonates, which may also interfere with the accurate determination of CEC. In this pretreatment, biochar−water mixtures were neutralized to pH 6.5 ± 0.02 by incremental additions of 0.5 M HCl and overnight shaking. The desired pH was obtained after 1 week, after which biochars were repeatedly washed until free of Cl^- as detected by $AgNO_3$ and dried at 50 °C for 5 days. Acid washing compared to only water leaching had little impact on the corncob biochar CEC, but it did reduce the miscanthus CEC by an average of 28%. Because the CEC of low-pH hydrochar was also reduced by 20% through acid washing, raising questions regarding the nature of the response, we chose a method that is less disruptive, namely, one without HCl washing.

Internal SA was measured using the Brunauer, Emmett, and Teller (BET) theory with N_2 as the adsorbate. Samples were dried at 106 °C for 90 min, milled, and then degassed in vacuum for 2 h at 120 or 150 °C: degassing temperature was chosen on the basis of sample HTT history. Measurements were performed on ca. 1 g samples on a NOVA 2000 (Quantachrome Instruments, Boynton Beach, FL, USA). The multipoint BET method was applied in the range of partial pressures of 0.05−0.30 P/P_0.

Statistics and Data Analysis. Multiple stepwise linear regressions and Spearman rank order correlations were performed with Sigmaplot version 11.0 (Systat Software Inc., San Jose, CA, USA).

RESULTS AND DISCUSSION

Yield and Proximate Analysis. Charcoal yield, VM content, and fixed carbon content changed nonlinearly in response to slow pyrolysis HTT (Figure 2). This type of nonlinear decrease in charcoal yield and VM and a corresponding increase in fixed carbon content are common biomass responses to increasing HTT.[5] Biochar yield and VM content responses to HTT were similar for the two feedstocks (Figure 2a,b). Eighty percent of VM loss occurred at 209−543 °C for corncob and at 241−509 °C for miscanthus. The VM contents of corncob and miscanthus feedstocks were similar, 81.1 and 78.0%, respectively. Despite the use of fairly similar C4 plants as feedstock, those being grass species of tropical origin, similar VM loss functions under pyrolysis were not necessarily obvious, as the two feedstocks differed somewhat in structural chemical composition. Our corncob and miscanthus feedstocks contained 13.8 and 21.3% lignin, respectively, as

dx.doi.org/10.1021/jf501139f | J. Agric. Food Chem. 2014, 62, 3791−3799

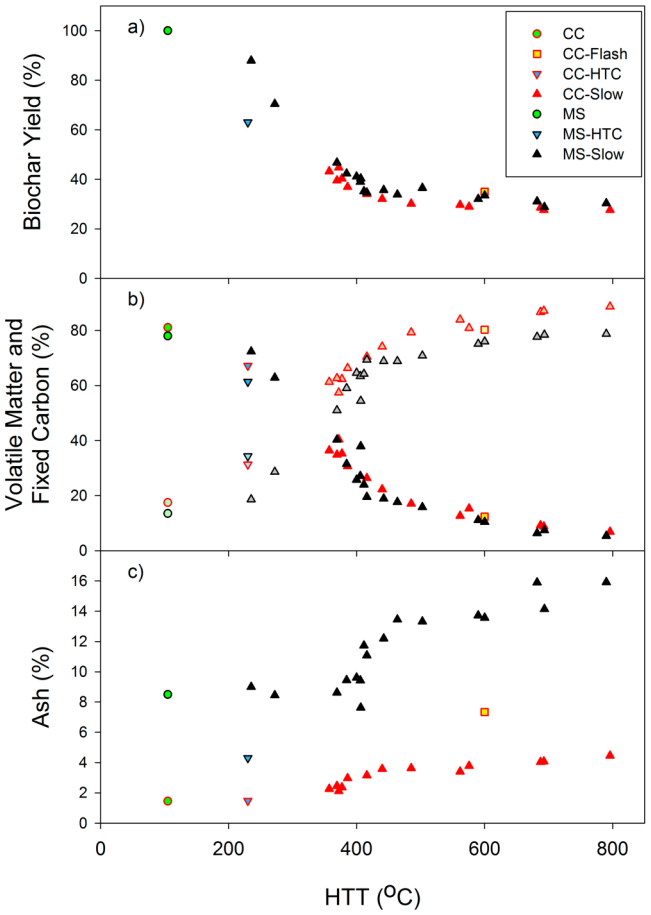

Figure 2. (a) Yield, (b) VM and fixed carbon (lighter fill) content, and (c) ash content as a function of highest treatment temperature (HTT) for corncob (CC), miscanthus (MS), and respective biochars produced through slow pyrolysis (Slow), flash carbonization (Flash), and hydrothermal carbonization (HTC). Reported biochar yield, VM, fixed carbon, and ash content are averages from three analytical replicates.

determined by advanced NMR investigations,[28] and these values are comparable to other reports of lignin in corncob and miscanthus: 14.7 and 23%, respectively.[19,29] Lignin content has been reported to affect biochar yield[30] due to the high C content of its constitutive polyphenol structure.[31] Additionally, mass loss during the pyrolysis process has been mainly attributed to degradation of cellulose at temperatures between 300 and 400 °C.[32] Our previous NMR investigations suggest that miscanthus had lower cellulose and hemicellulose contents than corncob but a higher degree of cellulose crystallinity.[28] Our results therefore suggest that the consistent biochar yield and VM contents obtained for grass-derived biochars hold across substantial variation in cellulose, hemicellulose, and lignin contents of feedstocks. The apparent absence of effect from variation in ash content and particle size would need to be confirmed with multiple grass feedstocks.

Hydrochars from HTC production displayed lower yield and VM content than slow pyrolysis biochars produced at similar HTT (Figure 2a,b). Although the hydrochars were produced at 230 °C, their VM and fixed C content were closer to those of 300 °C than of 250 °C slow pyrolysis biochars. On the basis of the amount of C recovered, Fuertes et al.[33] reported that 250 °C hydrochars are similar to slow pyrolysis biochars produced at nearly 400 °C. Our results confirm that HTC leads to a higher degree of carbonization than slow pyrolysis at comparable HTT. This is probably due to the reaction enhancement effects of pressure and the presence of water under HTC conditions. Flash carbonization HTT was not directly measured due to inhomogeneity within the reactor. The general relationship between VM and HTT for corncob (Figure 2b) suggests a production HTT for flash carbonization char between 520 and 640 °C. This temperature estimate is in the range of afterburner gas temperatures of the flash carbonizer.[34]

Ash in slow pyrolysis biochar became increasingly concentrated with increasing HTT (Figure 2c). Miscanthus hydrochar contained less ash than its feedstock, which is likely explained by mineral loss through the liquid phase during the HTC process. However, we did not observe a similar decrease in ash content for the corncob hydrochar, suggesting a feedstock-specific response. Contrasting trends in hydrochar ash content with different feedstocks were also found by Cao et al.[35] The ash content of feedstock used in flash carbonization was 6.3%, indicating that flash carbonization, like slow pyrolysis, leads to a concentration of ash. Only HTC produced a low-ash carbonization product.

Elemental Composition. Carbon and nitrogen were lost at a slower rate than oxygen and hydrogen during pyrolysis, resulting in their progressive concentration in the biochars with increasing pyrolysis HTT (Table 1). This effect has been well documented.[6] A Van Krevelen diagram relating H/C to O/C shows that the distribution of atomic ratios obtained from chars in this study was independent of feedstock and pyrolysis process (Figure 3). In our study, we directly measured O

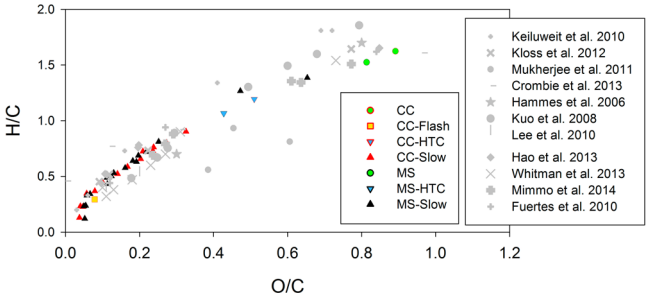

Figure 3. Van Krevelen diagram of samples analyzed in this study (in color) and literature values (gray) of grass feedstocks and biochars from 11 studies. Atomic ratios are averages from at least three analytical replicates.

contents, whereas most published studies report O values as calculated by subtracting the sum of C, H, N, and ash contents. Our measured values were more consistent than those we calculated by difference (data not shown), as the latter method combines the cumulative errors of all measurements. However, our O measurements for feedstocks were high, with O/C ratios between that of pure cellulose and sucrose. Despite the discrepancy at high O/C ratio, our atomic ratios obtained with measured O are remarkably consistent with literature values for grass-derived biochars obtained in 11 studies (Figure 3). It has been shown for biochars from a wide range of feedstocks that HTT plays a decisive role in causing the decrease in H/C and O/C ratios of produced biochar samples.[36] On the basis of the Van Krevelen plot, hydrochars and flash carbonization biochar appear equivalent to slow pyrolysis biochars produced at approximately 300 and 600 °C, respectively. This finding is

dx.doi.org/10.1021/jf501139f | J. Agric. Food Chem. 2014, 62, 3791−3799

consistent with the estimate of equivalent HTTs for chars from HTC and flash carbonization based on the relationship with VM. The independence of biochar elemental composition from feedstock and pyrolysis process is further confirmed by the consistent relationship between VM and molar ratios (Figure 4). Spokas[37] suggests that molar ratios encapsulate all

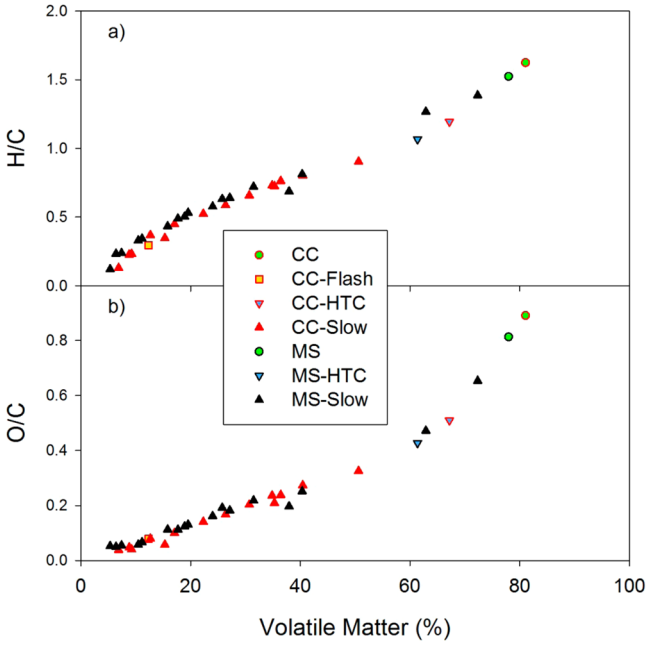

Figure 4. Atomic ratios (a) H/C and (b) O/C as a function of highest treatment temperature (HTT) for corncob (CC), miscanthus (MS), and respective biochars produced through slow pyrolysis (Slow), flash carbonization (Flash), and hydrothermal carbonization (HTC). Averages were obtained from at least three analytical replicates.

production parameters influencing carbonization. Other studies indicate that high-ash biochars such as those from food waste would require a combination of VM and atomic ratios for their characterization.[38] It has also been reported that H/C atomic ratios are not able to differentiate between the reactions occurring during HTC.[35] Our results suggest that both VM and atomic ratios can be used for characterizing the general charring history of grass-derived biochars. We further support the use of atomic ratios over volatile matter due to the stability of elemental composition measurements across studies as compared to proximate analysis.

Surface Property: pH. The pH of slow pyrolysis biochars increased with production HTT, reaching a plateau at approximately 450 °C (Figure 5a). Slow pyrolysis biochars produced above 450 °C had average pH that was 4.1 and 3.9 units higher than that of the corncob and miscanthus feedstocks, respectively. Flash carbonization biochar also had a pH that was 4.2 units above that of the feedstock. Our study shows that HTTs of 400−450 °C are sufficient for raising the biochar pH and producing C-rich biochar. Up to 7.6 pH unit increases have been shown in some biochars, with smaller increases in wood- and straw-derived biochars.[10] By contrast, HTC treatment significantly reduced the pH of the biomass by 1.3 and 2.4 units in corncob and miscanthus, respectively. Similar results were reported by Fuertes et al.,[33] who hypothesized that acidity in hydrochars may be due to a high content of carboxylic functional groups. The O/C atomic ratio, however, did not reflect the acidity of the hydrochars.

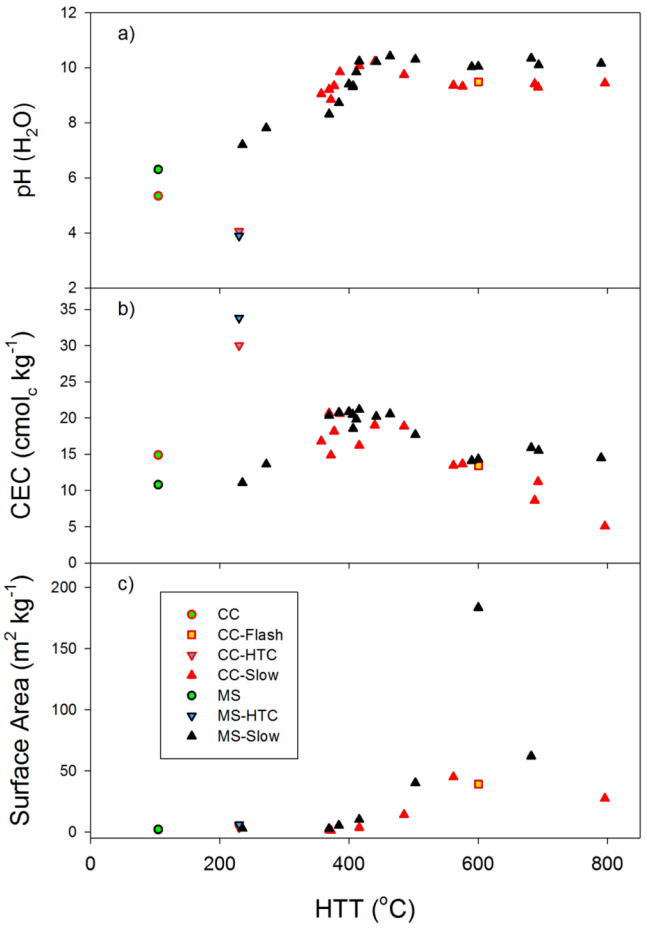

Figure 5. Surface properties (a) pH, (b) cation exchange capacity (CEC), and (c) surface area (SA), as a function of highest treatment temperature (HTT) for corncob (CC) and miscanthus (MS) and respective biochars produced through slow pyrolysis (Slow), flash carbonization (Flash), and hydrothermal carbonization (HTC). Analytical replicates, n, are (a) n = 1, (b) n = 3 for all with the exception of two points where n = 1 and 2, and (c) n = between 2 and 8.

A significant correlation was observed between pH and O/C ratio for the biochars in this study when hydrochars were excluded (Figure 6a, R^2 = 0.854). In addition, the pH was significantly correlated to VM across slow pyrolysis and flash carbonization biochars:

$$\mathrm{pH} = 10.63 - (0.049 \times \mathrm{VM}) \quad R^2 = 0.78 \qquad (1)$$

Alkalinity is caused by negatively charged organic groups, such as $-COO^-$ (carboxylate) and O^- (hydroxyl), and carbonates on the surface of biochar.[39] With increasing pyrolysis intensity, the number of acid functional groups (as carboxylic) decreases and the decrease is linearly correlated with the loss of volatile matter.[40] A decrease in surface acidic groups and a concomitant increase in surface basic groups with increasing HTT have been correlated to an increase in buffering capacity with HTT.[41] In addition to the decrease in acid functional groups, carbonates have been reported as a source of alkalinity for higher HTT biochars.[39] Here we obtained only a weak correlation between ash and pH (Table 2). Although we cannot exclude carbonate, the high correlation of pH with VM and corresponding weak correlation with ash content suggest that organic functional groups were the main determinant of the pH response with

dx.doi.org/10.1021/jf501139f | J. Agric. Food Chem. 2014, 62, 3791−3799

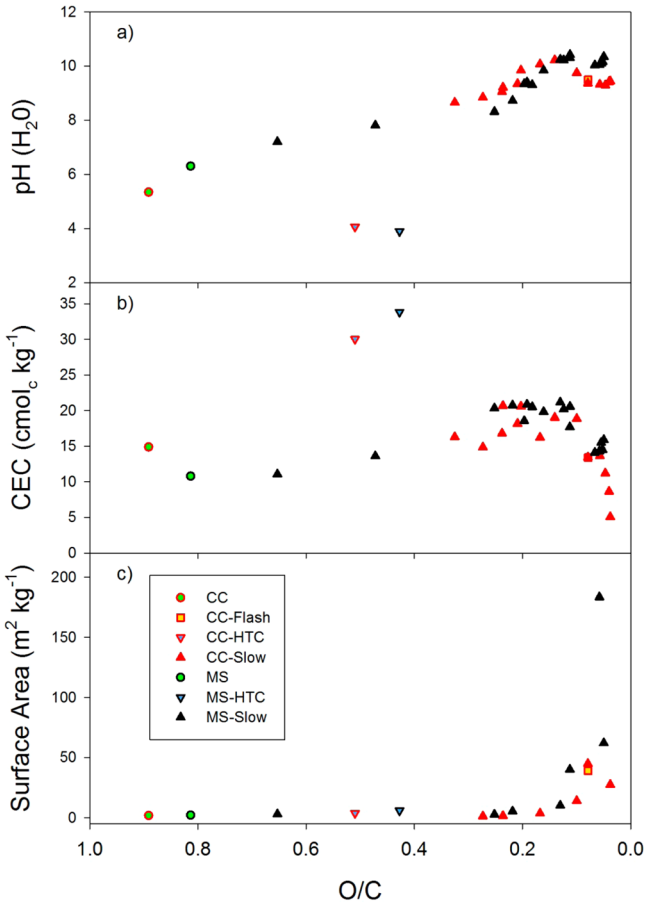

Figure 6. Surface properties (a) pH, (b) cation exchange capacity (CEC), and (c) surface area (SA) as a function of atomic ratio (O/C) for corncob (CC) and miscanthus (MS) and respective biochars produced through slow pyrolysis (Slow), flash carbonization (Flash), and hydrothermal carbonization (HTC). Analytical replicates, *n*, are (a) $n = 1$, (b) $n = 3$ for all with the exception of two points where $n = 1$ and 2, and (c) n = between 2 and 8.

HTT in slow pyrolysis biochars. Changes in pH as a function of the O/C ratio of slow pyrolysis biochars displayed a simple linear function, which did not fit the values of the hydrochars.

Surface Property: CEC. The CEC of both corncob and miscanthus slow pyrolysis biochars reached highest values at 350−475 °C (Figure 5b). The CEC of >450 °C biochars remained higher than that of feedstock for miscanthus while dropping substantially below for corncob. The lowest CEC was observed for the corncob sample pyrolyzed at 800 °C, suggesting that biochar CEC decreases with increasing HTT. Hydrochars displayed the highest CEC with an approximate doubling and tripling of CEC through HTC treatment of corncob and miscanthus, respectively. Flash carbonization, at an estimated 600 °C HTT, decreased the CEC of the feedstock only slightly, from 14.9 to 13.4 $cmol_c\ kg^{-1}$.

Values of H/C and O/C atomic ratios in biochars are reported to be positively correlated to concentration in hydroxyl, carboxyl, and carbonyl groups and thereby to CEC.[25,42] Our HTC chars, however, had similar H/C and O/C values but higher CEC than low-HTT slow pyrolysis biochars. The higher CEC of our HTC chars was therefore not clearly reflected in these atomic ratios. The relationship we found between the atomic ratio O/C and CEC of both HTC and slow pyrolysis chars is presented in Figure 6b. Only at O/C ratios below 0.1 did we observe a marked reduction in CEC for corncob biochars. Simple correlations between CEC and other individual parameters were weak (Table 2), and the correlation between CEC and O/C excluding HTC was even weaker (R^2 = 0.012). We found that it is not possible to infer CEC on the basis of production parameters or chemical composition tested in this study and, therefore, could not confirm our initial hypothesis.

Changes in CEC have previously been explained by the presence of acid functional groups (AFGs).[43] Using various feedstocks, Wang et al.[44] found consistently lower CEC of biochars produced at 700 °C as compared to 500 °C and a correlating decrease in acid functional groups at the higher HTT. More specifically, Harvey and colleagues[22] observed an increase in −OH functional groups at or above 300 °C HTT and a loss of carboxylic groups at HTT above 500 °C. Although Mukherjee, Zimmerman, and Harris[40] found a correlation between VM and AFGs for 250, 400, and 650 °C chars, they also observed a lack of correlation between CEC and VM seen in our data set. They explained that not all AFGs can function as cation exchange sites and that HTT affects CEC more than it does AFGs. Especially because of the drastically different behavior of the hydrochars, our study suggests that the CEC response is difficult to predict over a wide range of temperatures because it is influenced by multiple factors with none clearly dominating.

Surface Property: SA. The surface area of biochar did not increase significantly until the raw feedstock was treated at HTT above 400 °C as shown in Figure 5c. The highest SA value of 183 $m^2\ g^{-1}$ was obtained through pyrolysis of miscanthus at 600 °C, this value being nearly 2 orders of magnitude higher than that of the feedstock. Biochar SA decreased at pyrolysis HTTs above 600 °C, corresponding to

Table 2. Correlation Coefficients from Spearman Rank Order Correlation[a]

	HTT	ash	VM	H/C	O/C	CEC	SA	pH
HTT	1							
ash	0.46**	1						
VM	−0.98***	−0.51**	1					
H/C	−0.99***	−0.47**	0.99***	1				
O/C	−0.99***	−0.46**	0.99***	0.99***	1			
CEC	−0.40*	−0.01	0.31	0.34*	0.34*	1		
SA	0.79***	0.58*	−0.83***	−0.81***	−0.82***	−0.12	1	
pH	0.71***	0.52***	−0.75***	−0.73***	−0.72***	0.04	0.61**	1

[a] *n* is the lowest number of samples of the two analyses: $n = 35$ for temp, $n = 18$ for SA, and $n = 36$ for all other analyses. ***, **, and * indicate respective significance levels of 0.001, 0.01, and 0.05.

dx.doi.org/10.1021/jf501139f | J. Agric. Food Chem. 2014, 62, 3791−3799

O/C ratios below 0.2 (Figure 6c). HTC treatment did not increase SA, and this response is consistent with that of low-HTT slow pyrolysis biochars, both of which display high O/C ratios. The flash carbonization char exhibited a SA higher than most corncob chars in this study, and its SA appears to be similar to that of slow pyrolysis chars that underwent similar pyrolysis intensity.

Biochar SAs observed in this study are lower than values previously reported for corncob[45] and miscanthus[19] biochars of 300 and 400 $m^2 g^{-1}$. HTTs of 950 and 700 °C used to produce these respective biochars were also higher than those of the present study. Peak SA has been observed at HTTs between 650 and 850 °C for biochars from various feedstocks,[20] and HTTs >500 °C are needed to obtain significant increases in SA.[46] The increase in SA has been attributed mostly to the volatilization of organic compounds that otherwise clog pores,[42] similarly expressed in terms of loss of polar functional groups.[47] It has also been suggested that turbostratic structures harboring micropores develop through the growth of discontinuous graphene layers and that pore structures are destroyed at even higher temperatures when the turbostratic structures collapse into more organized graphite-like char.[48] Whereas HTT has been said to be the most important factor affecting SA,[49] the movement of volatiles away from char residues and the formation of cracks during pyrolysis are also influenced by carrier gas flow rate and other pyrolysis parameters involved with heat and mass transfer rates.[5,20] It is therefore not surprising that SA peaks and SA values at specific temperatures differ between studies, and although not all studies report a decrease in SA at higher HTT,[34,48] this effect might always be present if sufficiently high HTTs are applied. In our study, SA was poorly correlated to either VM content or O/C (Table 2), suggesting that the removal of VM from pores is not the only mechanism responsible for increased SA with increased HTT.

High SA, high CEC, and high pH are desirable properties of biochars for soil improvement. Here, as compared to feedstock, we increased SA by up to 2 orders of magnitude and pH by up to 4 units. In contrast, increases in CEC for slow pyrolysis remained modest irrespective of HTT. This finding suggests that designing a high-CEC biochar remains elusive, at least with the methods presently tested. This does not mean, however, that biochar transformations in soil cannot lead to improvement of soil CEC, as reported by Cheng et al.[43] Studies with wood-derived biochar suggested that concomitant increases in SA, CEC, and pH are obtained within a fairly narrow HTT range at around 400–450 °C.[18] Here, high SA was obtained only around 600 °C. This finding agrees with other grass-derived biochar studies which indicate that higher HTT is needed for obtaining high SA.[21] Proximate analysis and atomic ratios were poor predictors of SA and CEC, and our hypothesis that surface properties could be predicted from composition indicators was not confirmed. Specific production parameters appeared to have a significant impact on surface properties, indicating that specific analyses are necessary to identify and characterize high-SA biochars.

■ ASSOCIATED CONTENT

Supporting Information

Tables 1S and 2S. This material is available free of charge via the Internet at http://pubs.acs.org.

■ AUTHOR INFORMATION

Corresponding Author

*(A.B.) Phone: +47 954 79 226. E-mail: alice.budai@bioforsk.no.

Funding

Funding for the research was provided by the Research Council of Norway through the project "Advanced Techniques to Evaluate the Long-term Stability and Carbon Sequestration Potential of Different Types of Biochar", NFR197531.

Notes

The authors declare no competing financial interest.

■ ACKNOWLEDGMENTS

Hydrochar samples were prepared and provided by Markus Antonietti at the Max-Planck Institute for Colloids and Interfaces in Potsdam, Germany.

■ ABBREVIATIONS USED

VM, volatile matter; HTC, hydrothermal carbonization; CEC, cation exchange capacity; HTT, highest treatment temperature; SA, surface area

■ REFERENCES

(1) Lehmann, J.; Joseph, S. *Biochar for Environmental Management: An Introduction*; International Biochar Initiative: Westerville, OH, USA, 2009; pp 1–12.

(2) Spokas, K. A.; Cantrell, K. B.; Novak, J. M.; Archer, D. W.; Ippolito, J. A.; Collins, H. P.; Boateng, A. A.; Lima, I. M.; Lamb, M. C.; McAloon, A. J.; Lentz, R. D.; Nichols, K. A. Biochar: a synthesis of its agronomic impact beyond carbon sequestration. *J. Environ. Qual.* **2012**, *41*, 973–989.

(3) Manya, J. J. Pyrolysis for biochar purposes: a review to establish current knowledge gaps and research needs. *Environ. Sci. Technol.* **2012**, *46*, 7939–7954.

(4) Shafizadeh, F. The chemistry of pyrolysis and combustion. *Adv. Chem. Ser.* **1984**, *No. 207*, 491–529.

(5) Antal, M. J.; Gronli, M. The art, science, and technology of charcoal production. *Ind. Eng. Chem. Res.* **2003**, *42*, 1619–1640.

(6) Neves, D.; Thunman, H.; Matos, A.; Tarelho, L.; Gomez-Barea, A. Characterization and prediction of biomass pyrolysis products. *Prog. Energy Combust. Sci.* **2011**, *37*, 611–630.

(7) Lehmann, J.; Gaunt, J.; M, R. Bio-char sequestration in terrestrial ecosystems – a review. *Mitigation Adaptation Strategies Global Change* **2006**, *11*, 403–427.

(8) Glaser, B.; Lehmann, J.; Zech, W. Ameliorating physical and chemical properties of highly weathered soils in the tropics with charcoal – a review. *Biol. Fertil. Soils* **2002**, *35*, 219–230.

(9) Jeffery, S.; Verheijen, F. G. A.; van der Velde, M.; Bastos, A. C. A quantitative review of the effects of biochar application to soils on crop productivity using meta-analysis. *Agric. Ecosyst. Environ.* **2011**, *144*, 175–187.

(10) Ronsse, F.; van Hecke, S.; Dickinson, D.; Prins, W. Production and characterization of slow pyrolysis biochar: influence of feedstock type and pyrolysis conditions. *Global Change Biol. Bioenergy* **2013**, *5*, 104–115.

(11) Ippolito, J. A.; Laird, D. A.; Busscher, W. J. Environmental benefits of biochar. *J. Environ. Qual.* **2012**, *41*, 967–972.

(12) Ameloot, N.; Graber, E. R.; Verheijen, F. G. A.; De Neve, S. Interactions between biochar stability and soil organisms: review and research needs. *Eur. J. Soil Sci.* **2013**, *64*, 379–390.

(13) McCormack, S. A.; Ostle, N.; Bardgett, R. D.; Hopkins, D. W.; Vanbergen, A. J. Biochar in bioenergy cropping systems: impacts on soil faunal communities and linked ecosystem processes. *Global Change Biol. Bioenergy* **2013**, *5*, 81–95.

(14) Liang, B.; Lehmann, J.; Solomon, D.; Kinyangi, J.; Grossman, J.; O'Neill, B.; Skjemstad, J. O.; Thies, J.; Luizao, F. J.; Petersen, J.; Neves,

E. G. Black carbon increases cation exchange capacity in soils. *Soil Sci. Soc. Am. J.* **2006**, *70*, 1719−1730.
(15) Laird, D. A.; Fleming, P.; Davis, D. D.; Horton, R.; Wang, B. Q.; Karlen, D. L. Impact of biochar amendments on the quality of a typical Midwestern agricultural soil. *Geoderma* **2010**, *158*, 443−449.
(16) Van Zwieten, L.; Kimber, S.; Morris, S.; Chan, K. Y.; Downie, A.; Rust, J.; Joseph, S.; Cowie, A. Effects of biochar from slow pyrolysis of papermill waste on agronomic performance and soil fertility. *Plant Soil* **2010**, *327*, 235−246.
(17) Budai, A.; Zimmerman, A. R.; Cowie, A. L.; Webber, J. B. W.; Singh, B. P.; Glaser, B.; Masiello, C. A.; Andersson, D.; Shields, F.; Lehmann, J.; Camps Arbestain, M.; Williams, M.; Sohi, S.; Joseph, S. *Biochar Carbon Stability Test Method: An Assessment of Methods To Determine Biochar Carbon Stability*; International Biochar Initiative (IBI): Westerville, OH, USA, 2013.
(18) Lehmann, J. Bio-energy in the black. *Front. Ecol. Environ.* **2007**, *5*, 381−387.
(19) Lee, Y.; Eum, P. R. B.; Ryu, C.; Park, Y. K.; Jung, J. H.; Hyun, S. Characteristics of biochar produced from slow pyrolysis of Geodae-Uksae 1. *Bioresour. Technol.* **2013**, *130*, 345−350.
(20) Brown, R. A.; Kercher, A. K.; Nguyen, T. H.; Nagle, D. C.; Ball, W. P. Production and characterization of synthetic wood chars for use as surrogates for natural sorbents. *Org. Geochem.* **2006**, *37*, 321−333.
(21) Chun, Y.; Sheng, G. Y.; Chiou, C. T.; Xing, B. S. Compositions and sorptive properties of crop residue-derived chars. *Environ. Sci. Technol.* **2004**, *38*, 4649−4655.
(22) Harvey, O. R.; Herbert, B. E.; Kuo, L. J.; Louchouarn, P. Generalized two-dimensional perturbation correlation infrared spectroscopy reveals mechanisms for the development of surface charge and recalcitrance in plant-derived biochars. *Environ. Sci. Technol.* **2012**, *46*, 10641−10650.
(23) Houben, D.; Sonnet, P.; Cornelis, J. T. Biochar from miscanthus: a potential silicon fertilizer. *Plant Soil* **2014**, *374*, 871−882.
(24) Wang, L.; Trninic, M.; Skreiberg, O.; Gronli, M.; Considine, R.; Antal, M. J. Is elevated pressure required to achieve a high fixed-carbon yield of charcoal from biomass? Part 1: Round-robin results for three different corncob materials. *Energy Fuels* **2011**, *25*, 3251−3265.
(25) Wiedner, K.; Naisse, C.; Rumpel, C.; Pozzi, A.; Wieczorek, P.; Glaser, B. Chemical modification of biomass residues during hydrothermal carbonization − what makes the difference, temperature or feedstock? *Org. Geochem.* **2013**, *54*, 91−100.
(26) Antal, M. J.; Mochidzuki, K.; Paredes, L. S. Flash carbonization of biomass. *Ind. Eng. Chem. Res.* **2003**, *42*, 3690−3699.
(27) Gaskin, J. W.; Steiner, C.; Harris, K.; Das, K. C.; Bibens, B. Effect of low-temperature pyrolysis conditions on biochar for agricultural use. *Trans. ASABE* **2008**, *51*, 2061−2069.
(28) Calucci, L.; Rasse, D. P.; Forte, C. Solid-state nuclear magnetic resonance characterization of chars obtained from hydrothermal carbonization of corncob and miscanthus. *Energy Fuels* **2013**, *27*, 303−309.
(29) Vassilev, S. V.; Baxter, D.; Andersen, L. K.; Vassileva, C. G.; Morgan, T. J. An overview of the organic and inorganic phase composition of biomass. *Fuel* **2012**, *94*, 1−33.
(30) Demirbas, A. Effects of temperature and particle size on bio-char yield from pyrolysis of agricultural residues. *J. Anal. Appl. Pyrolysis* **2004**, *72*, 243−248.
(31) Antal, M. J.; Allen, S. G.; Dai, X. F.; Shimizu, B.; Tam, M. S.; Gronli, M. Attainment of the theoretical yield of carbon from biomass. *Ind. Eng. Chem. Res.* **2000**, *39*, 4024−4031.
(32) Ascough, P. L.; Bird, M. I.; Wormald, P.; Snape, C. E.; Apperley, D. Influence of production variables and starting material on charcoal stable isotopic and molecular characteristics. *Geochim. Cosmochim. Acta* **2008**, *72*, 6090−6102.
(33) Fuertes, A. B.; Arbestain, M. C.; Sevilla, M.; Macia-Agullo, J. A.; Fiol, S.; Lopez, R.; Smernik, R. J.; Aitkenhead, W. P.; Arce, F.; Macias, F. Chemical and structural properties of carbonaceous products obtained by pyrolysis and hydrothermal carbonisation of corn stover. *Aust. J. Soil Res.* **2010**, *48*, 618−626.
(34) Nunoura, T.; Wade, S. R.; Bourke, J. P.; Antal, M. J. Studies of the flash carbonization process. 1. Propagation of the flaming pyrolysis reaction and performance of a catalytic afterburner. *Ind. Eng. Chem. Res.* **2006**, *45*, 585−599.
(35) Cao, X.; Ro, K. S.; Libra, J. A.; Kammann, C. I.; Lima, I.; Berge, N.; Li, L.; Li, Y.; Chen, N.; Yang, J.; Deng, B.; Mao, J. Effects of biomass types and carbonization conditions on the chemical characteristics of hydrochars. *J. Agric. Food Chem.* **2013**, *61*, 9401−9411.
(36) Mukome, F. N. D.; Zhang, X. M.; Silva, L. C. R.; Six, J.; Parikh, S. J. Use of chemical and physical characteristics to investigate trends in biochar feedstocks. *J. Agric. Food Chem.* **2013**, *61*, 2196−2204.
(37) Spokas, K. A. Review of the stability of biochar in soils: predictability of O:C molar ratios. *Carbon Manage.* **2010**, *1*, 289−303.
(38) Enders, A.; Hanley, K.; Whitman, T.; Joseph, S.; Lehmann, J. Characterization of biochars to evaluate recalcitrance and agronomic performance. *Bioresour. Technol.* **2012**, *114*, 644−653.
(39) Yuan, J. H.; Xu, R. K.; Zhang, H. The forms of alkalis in the biochar produced from crop residues at different temperatures. *Bioresour. Technol.* **2011**, *102*, 3488−3497.
(40) Mukherjee, A.; Zimmerman, A. R.; Harris, W. Surface chemistry variations among a series of laboratory-produced biochars. *Geoderma* **2011**, *163*, 247−255.
(41) Al-Wabel, M. I.; Al-Omran, A.; El-Naggar, A. H.; Nadeem, M.; Usman, A. R. A. Pyrolysis temperature induced changes in characteristics and chemical composition of biochar produced from conocarpus wastes. *Bioresour. Technol.* **2013**, *131*, 374−379.
(42) Lee, J. W.; Kidder, M.; Evans, B. R.; Paik, S.; Buchanan, A. C.; Garten, C. T.; Brown, R. C. Characterization of biochars produced from cornstovers for soil amendment. *Environ. Sci. Technol.* **2010**, *44*, 7970−7974.
(43) Cheng, C. H.; Lehmann, J.; Thies, J. E.; Burton, S. D.; Engelhard, M. H. Oxidation of black carbon by biotic and abiotic processes. *Org. Geochem.* **2006**, *37*, 1477−1488.
(44) Wang, Y.; Hu, Y.; Zhao, X.; Wang, S.; Xing, G. Comparisons of biochar properties from wood material and crop residues at different temperatures and residence times. *Energy Fuels* **2013**, *27*, 5890−5899.
(45) Bourke, J.; Manley-Harris, M.; Fushimi, C.; Dowaki, K.; Nunoura, T.; Antal, M. J. Do all carbonized charcoals have the same chemical structure? 2. A model of the chemical structure of carbonized charcoal. *Ind. Eng. Chem. Res.* **2007**, *46*, 5954−5967.
(46) Kloss, S.; Zehetner, F.; Dellantonio, A.; Hamid, R.; Ottner, F.; Liedtke, V.; Schwanninger, M.; Gerzabek, M. H.; Soja, G. Characterization of slow pyrolysis biochars: effects of feedstocks and pyrolysis temperature on biochar properties. *J. Environ. Qual.* **2012**, *41*, 990−1000.
(47) Chen, B. L.; Zhou, D. D.; Zhu, L. Z. Transitional adsorption and partition of nonpolar and polar aromatic contaminants by biochars of pine needles with different pyrolytic temperatures. *Environ. Sci. Technol.* **2008**, *42*, 5137−5143.
(48) Keiluweit, M.; Nico, P. S.; Johnson, M. G.; Kleber, M. Dynamic molecular structure of plant biomass-derived black carbon (biochar). *Environ. Sci. Technol.* **2010**, *44*, 1247−1253.
(49) Lua, A. C.; Yang, T.; Guo, J. Effects of pyrolysis conditions on the properties of activated carbons prepared from pistachio-nut shells. *J. Anal. Appl. Pyrolysis* **2004**, *72*, 279−287.
(50) Crombie, K.; Masek, O.; Sohi, S. P.; Brownsort, P.; Cross, A. The effect of pyrolysis conditions on biochar stability as determined by three methods. *Global Change Biol. Bioenergy* **2013**, *5*, 122−131.
(51) Hammes, K.; Smernik, R. J.; Skjemstad, J. O.; Herzog, A.; Vogt, U. F.; Schmidt, M. W. I. Synthesis and characterisation of laboratory-charred grass straw (*Oryza sativa*) and chestnut wood (*Castanea sativa*) as reference materials for black carbon quantification. *Org. Geochem.* **2006**, *37*, 1629−1633.
(52) Kuo, L. J.; Herbert, B. E.; Louchouarn, P. Can levoglucosan be used to characterize and quantify char/charcoal black carbon in environmental media? *Org. Geochem.* **2008**, *39*, 1466−1478.

(53) Hao, F. H.; Zhao, X. C.; Ouyang, W.; Lin, C. Y.; Chen, S. Y.; Shan, Y. S.; Lai, X. H. Molecular structure of corncob-derived biochars and the mechanism of atrazine sorption. *Agron. J.* **2013**, *105*, 773−782.
(54) Mimmo, T.; Panzacchi, P.; Baratieri, M.; Davies, C. A.; Tonon, G. Effect of pyrolysis temperature on miscanthus (*Miscanthus* × *giganteus*) biochar physical, chemical and functional properties. *Biomass Bioenergy* **2014**, 10.1016/j.biombioe.2014.01.004.
(55) Whitman, T.; Hanley, K.; Enders, A.; Lehmann, J. Predicting pyrogenic organic matter mineralization from its initial properties and implications for carbon management. *Org. Geochem.* **2013**, *64*, 76−83.

Table 1S: Biochar composition from proximate analysis and surface properties of corncob (CC) and miscanthus (MS) exposed to hydrothermal carbonization (HTC), slow pyrolysis (Slow), and flash carbonization (Flash) at designated highest treatment temperatures (HTT)[a]

feedstock – method	HTT	yield	VM		fC	ash		pH	SA	
	°C	%	%		%	%		in H_2O	$m^2 g^{-1}$	
CC	105	100	81.1	(0.5)	17.5	1.5	(0.0)	5.3	1.8	(0.1)
CC-Flash	600	35	12.3	(0.1)	80.3	7.3	(0.7)	9.5	39.1	(2.9)
CC-HTC	230	63	67.2	(0.1)	31.3	1.5	(0.2)	4.1	3.8	(0.1)
CC-Slow	230	52	50.6	(0.1)	47	2.4	(0.0)	8.7		
CC-Slow	377	40	35.3	(0.2)	62.3	2.4	(0.4)	9.3		
CC-Slow	372	45	40.5	(0.1)	57.4	2.1	(0.0)	8.8	1.3	(0.4)
CC-Slow	369	40	34.8	(1.0)	62.7	2.5	(0.1)	9.2	1.5	(0.2)
CC-Slow	357	43	36.4	(0.5)	61.3	2.3	(0.2)	9.1		
CC-Slow	386	37	30.7	(0.3)	66.3	3	(0.3)	9.8	1.63	(0.4)
CC-Slow	416	34	26.4	(0.2)	70.5	3.2	(0.1)	10.1	3.6	(0.9)
CC-Slow	440	32	22.3	(0.2)	74.1	3.6	(0.3)	10.2		
CC-Slow	485	30	17.1	(0.2)	79.3	3.6	(0.4)	9.8	14.1	(3.0)
CC-Slow	562	30	12.7	(0.1)	83.9	3.4	(0.2)	9.4	44.9	(3.2)
CC-Slow	576	29	15.3	(4.1)	80.9	3.8	(0.1)	9.3		
CC-Slow	687	29	9.2	(1.2)	86.7	4	(0.1)	9.4		
CC-Slow	693	28	8.8	(0.7)	87.1	4.1	(0.1)	9.3		
CC-Slow	796	28	6.9	(0.1)	88.7	4.5	(0.1)	9.4	27.4	(2.8)
MS	105	100	78	(0.8)	13.5	8.5	(0.4)	6.3	2.1	(0.4)
MS-HTC	230	63	61.4	(0.9)	34.3	4.3	(1.1)	3.9	5.9	(0.1)
MS-Slow	272	70	62.9	(0.2)	28.7	8.4	(0.2)	7.8		
MS-Slow	235	88	72.4	(1.9)	18.6	9	(0.7)	7.2	2.9	(0.0)
MS-Slow	369	47	40.4	(0.3)	51	8.6	(0.9)	8.3	2.7	(0.2)
MS-Slow	385	42	31.5	(0.7)	59.1	9.4	(0.5)	8.7	5.3	(0.5)
MS-Slow	400	41	25.8	(0.2)	64.6	9.6	(0.4)	9.4		
MS-Slow	406	39	27.1	(0.2)	63.4	9.4	(0.4)	9.3		
MS-Slow	411	35	24.0	(1.5)	64.2	11.7	(1.7)	9.8		

MS-Slow	406	40	38.0	(9.3)	54.4	7.6	(0.6)	9.3		
MS-Slow	416	35	19.6	(0.4)	69.4	11.1	(1.6)	10.2	10.1	(0.5)
MS-Slow	442	36	18.9	(0.3)	68.9	12.2	(0.8)	10.2		
MS-Slow	503	36	15.8	(0.6)	70.9	13.3	(0.2)	10.3	40.1	(1.8)
MS-Slow	464	34	17.7	(0.2)	68.9	13.5	(0.3)	10.4		
MS-Slow	600	33	10.5	(1.3)	76.0	13.6	(0.8)	10.0	183.3	(23.2)
MS-Slow	590	32	11.1	(2.4)	75.1	13.7	(1.5)	10.0		
MS-Slow	693	29	7.4	(0.2)	78.4	14.1	(1.3)	10.1		
MS-Slow	682	31	6.4	(0.4)	77.7	15.9	(0.8)	10.3	62	(3.9)
MS-Slow	790	30	5.3	(1.2)	78.8	15.9	(0.4)	10.2		

Standard Deviations are shown in parentheses for analytical replicates; n=3 for volatile matter (VM), fixed carbon (fC), and ash which were obtained on a dry weight % basis, n=2–8 for surface are (SA), and n=1 for pH.

Table 2S: Cation exchange capacity (CEC) calculated from the sum of cations calcium (Ca), potassium (K), magnesium (Mg), sodium (Na), and hydrogen (H) where pH>7.

feedstock – method	HTT	CEC		Ca	K	Mg	Na	H
	°C				$cmol_c\ kg^{-1}$			
CC	105	14.9	(0.5)	0.7	3.5	2.2	0.1	8.3
CC-Flash	600	13.4	(0.4)	0.6	11.0	1.7	0.1	0.0
CC-HTC	230	30.0	(0.5)	0.2	0.2	0.1	0.0	29.5
CC-Slow	230	16.3	(0.8)	0.3	15.1	0.7	0.2	0.0
CC-Slow	377	18.2	(0.6)	0.3	17.2	0.6	0.0	0.0
CC-Slow	372	14.9	(0.6)	0.2	14.4	0.3	0.1	0.0
CC-Slow	369	20.7	(0.2)	0.4	19.5	0.7	0.1	0.0
CC-Slow	357	16.8	(0.2)	0.7	15.2	0.7	0.2	0.0
CC-Slow	386	20.6	(0.3)	0.4	19.6	0.6	0.0	0.0
CC-Slow	416	16.2	(0.5)	0.2	15.7	0.3	0.0	0.0
CC-Slow	440	19.0	(1.4)	0.2	18.5	0.3	0.0	0.0
CC-Slow	485	18.9	(1.2)	0.2	18.5	0.2	0.0	0.0
CC-Slow	562	13.5	(1.3)	0.2	12.9	0.3	0.0	0.0
CC-Slow	576	13.7	(0.5)	0.2	13.2	0.2	0.0	0.0
CC-Slow	687	8.6	(0.3)	0.3	7.9	0.4	0.0	0.0
CC-Slow	693	11.2	(0.9)	0.3	10.6	0.2	0.1	0.0
CC-Slow	796	5.1	(0.0)''	0.3	4.5	0.3	0.1	0.0
MS	105	10.8	(0.2)	2.8	1.2	1.6	0.1	5.2
MS-HTC	230	33.8	(0.4)	0.4	0.3	0.1	0.1	33.0
MS-Slow	272	13.6	'	5.6	6.4	1.4	0.2	0.0
MS-Slow	235	11.1	(0.7)	5.3	3.6	1.8	0.1	0.3
MS-Slow	369	20.3	(0.4)	6.0	12.4	1.7	0.3	0.0
MS-Slow	385	20.8	(0.5)	6.5	12.4	1.5	0.3	0.0
MS-Slow	400	20.9	(0.2)	6.5	12.6	1.5	0.3	0.0
MS-Slow	406	20.5	(0.4)	5.6	13.2	1.4	0.2	0.0
MS-Slow	411	19.8	(0.2)	5.6	12.5	1.5	0.2	0.0
MS-Slow	406	18.6	(1.0)	4.7	12.2	1.4	0.2	0.0
MS-Slow	416	21.2	(0.5)''	6.4	13.0	1.6	0.2	0.0

MS-Slow	442	20.2	(0.3)	6.5	12.0	1.5	0.2	0.0
MS-Slow	503	17.7	(0.5)	5.9	10.5	1.2	0.2	0.0
MS-Slow	464	20.6	(0.9)	6.4	12.4	1.6	0.2	0.0
MS-Slow	600	14.3	(0.1)	5.5	7.7	1.0	0.1	0.0
MS-Slow	590	14.1	(0.4)	4.8	8.1	1.0	0.2	0.0
MS-Slow	693	15.5	(0.1)	5.2	8.8	1.3	0.2	0.0
MS-Slow	682	15.9	(0.3)	7.8	6.4	1.5	0.2	0.0
MS-Slow	790	14.5	(0.2)	8.5	4.4	1.4	0.2	0.0

Standard Deviations are shown in parentheses for analytical replicates; n=3 for cation exchange capacity (CEC) with the exception of two points, ' and '', where n=1 and 2, respectively.